# Compensatory Mutations Restore Fitness During the Evolution of Dihydrofolate Reductase

# Compensatory mutations restore fitness during the evolution of dihydrofolate reductase

Kyle M Brown[1]*, Marna Costanzo[1], Wenxin Xu[1], Scott Roy[2] and Daniel L Hartl[1]

[1]Department of Organismic and Evolutionary Biology, Harvard University, 16 Divinity Avenue, Cambridge, MA 02138

[2]National Center for Biotechnology Information (NCBI), National Library of Medicine (NLM), National Institutes of Health (NIH), Bldg. 38A Room 5N503, 8600 Rockville Pike, Bethesda, MD 20894

*Corresponding Author: Kyle M. Brown, Harvard University, 16 Divinity Avenue, Cambridge, MA 02138, Phone: 617-496-5540, Fax: 617-496-5854, kylemichaelbrown@gmail.com

Keywords: drug resistance, malaria, phenotypic robustness, mutational landscapes, compensatory mutations

**Abstract**

Whether a trade-off exists between robustness and evolvability is an important issue for protein evolution. While traditional viewpoints have assumed that existing functions must be compromised by the evolution of novel activities, recent research has suggested that existing phenotypes can be robust to the evolution of novel protein functions. Enzymes that are targets of antibiotics that are competitive inhibitors must evolve decreased drug affinity while maintaining their function and sustaining growth. Utilizing a transgenic *Saccharomyces cerevisiae* model expressing the dihydrofolate reductase (DHFR) enzyme from the malarial parasite *Plasmodium falciparum*, we examine the robustness of growth rate to drug-resistance mutations. We assay the growth rate and resistance of all 48 combinations of 6 DHFR point mutations associated with increased drug resistance in field isolates of the parasite. We observe no consistent relationship between growth and resistance phenotypes among the DHFR alleles. The three evolutionary pathways that dominate DHFR evolution show that mutating with increased resistance can compensate for initial declines in growth rate from previously acquired mutations. In other words, resistance mutations that occur later in evolutionary trajectories can compensate for the fitness consequences of earlier mutations. Our results suggest that high levels of resistance may be selected for without necessarily jeopardizing overall fitness.

## Introduction

In protein evolution, the development of a new function is often thought to necessitate the deterioration of an existing function (Kondrashov 2005). Such potential trade-offs would constrain protein evolution and slow the emergence of new protein functions. However, recent research has suggested that proteins may be phenotypically robust and capable of evolving novel functions without compromising existing activities (Aharoni et al. 2005, Tawfik 2005, Khersonsky et al. 2006).

Enzymes that are targeted by competitive inhibitors must evolve decreased affinity for the antibiotic while maintaining their initial catalytic ability(s). For example, enzymes in human pathogens such as *Streptococcus, Staphylococus*, and HIV have evolved decreased antibiotic susceptibility via a series of point mutations while maintaining their original functions (e.g. Laible et al. 1989, Hackbarth et al. 1995, Berkhout 1999). However, sometimes such resistance mutations impose fitness costs, as in the case of a ribosomal protein in *Salmonella* (Björkman et al. 1998, Maisnier-Paitin et al. 2002, Maisnier-Paitin and Andersson 2004). In view of the antibiotic "warfare" among organisms that began long before the onset of anthropogenic drug pressure, antibiotic resistance is not only a threat to human health, but also raises fundamental evolutionary questions (e.g. Maplestone et al. 1992, Currie et al. 1999).

In order to understand whether phenotypic tradeoffs exist and how they affect protein evolution, we chose a well-characterized enzyme whose evolution has been recently shaped by antibiotic pressure. Dihydrofolate reductase (DHFR) plays an important role in the folate pathway, helping to provide cofactors for several important cellular reactions including DNA synthesis (Nirmalan et al. 2002). In *Plasmodium falciparum*, the parasite responsible for the deadliest form of malaria, DHFR is the target of antifolate drugs, which represent inexpensive

and potentially effective malarial therapies (Schlitzer 2007). Increased use of antifolate drugs, particularly pyrimethamine, has selected for antifolate resistant DHFR alleles. Several mutations at the DHFR locus of *P. falciparum* are now associated with high-level pyrimethamine resistance in field isolates (e.g. Sirawaraporn et al. 1997, Ekland and Fidlock 2007, Mita et al. 2007).

Using a transgenic *Saccharomyces cerevisiae* model of *P. falciparum* antifolate resistance (Sibley and Macreadie 2001), we explored the mutational landscape of pyrimethamine resistance in DHFR. We followed the combinatorial strategy of Weinreich et al. (2006) and constructed all 48 combinations of 6 mutations at 5 amino acid sites. Each of these mutations is associated with pyrimethamine resistance and has been observed in combination with one or more of the other 5 mutations in malarial field isolates (Foote et al. 1990, Sirawaraporn et al. 1997). We observe a single fitness maximum which population genetic simulations suggest is most likely to be accessible by a small number of mutational paths. These pathways exhibit compensatory evolution: initial resistance-conferring mutations decrease growth rate, however their effects are quickly compensated for by subsequent mutations. Our results suggest that high levels of resistance may be selected for without necessarily jeopardizing overall fitness.

## Methods

*Yeast Strain Construction*

Carol Sibley of the University of Washington generously provided the GR7 shuttle vector, a derivative of the pRS314 yeast shuttle vector (Sikorski and Hieter 1989, Wooden et al. 1997). This vector contains the wild-type *P. falciparum DHFR* allele regulated by 600 base pairs from the promoter region of the *S. cerevisiae DFR1* gene and by the 400 base pair 3' *DFR1* transcription and translation terminators. GR7 also includes the *TRP1* yeast biosynthetic marker, and a yeast centromere sequence that maintains the plasmid at about one copy per cell (Hunt et al. 2005).

We constructed all 48 possible combinations of the 6 point mutations at 5 amino acid coding sites in *DHFR* (A16V, N51I, C59R, S108N/T, I164L) on the GR7 vector using the QuikChange Site-Directed Mutagenesis Kit (Stratagene, Cedar Creek TX). The *DHFR* locus on each mutagenized plasmid was sequenced to verify the presence of the engineered mutations.

We used the *S. cerevisiae* strain TH5 (*MATa leu2-3,112 trp1 ura3-52 dfr1::URA3 tup1*; provided by Carol Sibley) to assay the level of pyrimethamine resistance conferred by each *DHFR* allele. TH5 lacks *DFR1*, the yeast orthologue of the *DHFR* gene and, when not transformed with a functional *DFR1* homolog, the strain requires media supplemented with 100μg/mL deoxythymidine monophosphate (dTMP; Sigma-Alrich, St. Louis, MO) for growth. The *tup1* mutation increases cellular permeability to dTMP (Wooden et al. 1997). We transformed TH5 with each of the 48 alleles using the EZ Yeast Transformation Kit (Zymo, Orange CA), selecting for the presence of the GR7 vector on tryptophan dropout media (SC trp-) supplemented with 100μg/mL dTMP.

*Minimum Inhibitory Concentrations*

Minimum inhibitory concentrations (MICs) for pyrimethamine were determined using a solid plate assay. For each biological replicate of each strain, a colony was picked into 3 ml unsupplemented liquid YPD. After 48 hours, we measured optical density ($OD_{600}$), and each strain was serially diluted to a final $OD_{600}$ of 0.002 (~$1.2x10^4$ cells/ml). Five µl of each diluted strain (~60 cells) was spotted on plates containing either ethanol (negative control) or increasing concentrations of pyrimethamine. We used two biological replicates each with four technical replicates for each strain. The minimum inhibitory concentration (MIC) for each replicate was defined as the lowest concentration of pyrimethamine to fully inhibit growth.

Strains were initially assayed using a $\log_{10}$ scale of pyrimethamine concentrations, ranging from $10^{-9}$ to $10^{-4}$ M. To further resolve MIC values among strains, we used additional pyrimethamine concentrations ($2.5 \times 10^{-a}$, $5 \times 10^{-a}$, and $7.5 \times 10^{-a}$ between each set of concentrations $10^{-(a+1)}$ and $10^{-a}$) for all strains with MIC values higher than $10^{-6}$ M. The full MIC data set is listed in Supplementary Table S4.

*Growth Rate Measurements*

Following Joseph and Hall (2004), we measured the growth rate of each strain in the presence various concentrations of pyrimethamine (0 M, $10^{-8}$ M, $10^{-7}$ M, $10^{-6}$ M, $10^{-5}$ M, $10^{-4}$ M) using a Bioscreen C microbiological workstation (Thermo Labsystems). For each biological replicate, we picked a colony from a solid media plate and inoculated a 5 ml liquid YPD culture. After 48 hours of shaking incubation at 30˚C, cultures were diluted to an optical density ($OD_{600}$) of 0.01, or approximately $6 * 10^4$ cells/mL. Aliquots of 200 µl were transferred to microtiter

plates for growth in the Bioscreen, and the optical density ($OD_{600}$) was measured every 15 minutes for 3 days. For each of at least 2 biological replicates per strain, we assayed at least 4 technical replicates in each concentration of pyrimethamine. Using code written in *R*, we calculated least-squares linear regressions for log absorbance versus time for a 3.25-hour sliding window over the length of the growth curve. Growth rates represent the maximum regression coefficient among all sliding windows over length of the growth curve. Growth rates of each allele in the absence of pyrimethamine are depicted in Supplementary Table S2.

*IC50 calculations*

For each strain, we fit the following logarithmic curve to our growth rate versus pyrimethamine concentration data:

$$G_i = \frac{A_i}{1 + e^{\frac{b_i - x}{c_i}}} \quad (1)$$

where $G_i$ is the growth rate of strain *i*, $A_i$ is the maximum growth rate in the absence of pyrimethamine, $b_i$ is the pyrimethamine concentration where $G_i$ is half of $A_i$, $c_i$ is a scaling parameter determining the shape of the logistic regression, and $x$ is the $\log_{10}$ of the pyrimethamine concentration. IC50 values for each strain represent the value of $b_i$ from nonlinear least-squares regressions. Regression code was written in *R*.

We determined the correlation between our calculated IC50 values and our observed MICs (Spearman's rank correlation: $P = 5.895 * 10^{-11}$, Figure S1). For three *DHFR* alleles (C59R/S108N/I164L, N51I/S108N/I164L, N51I/C59R/S108N/I164L), statistically significant IC50 values could not be determined from our logistic regressions because we did not observe a

significant decrease in growth rate over the range of pyrimethamine concentrations. For these cases, we fit a linear model (IC50~MIC) to our resistance data and used this model to predict the IC50 values of the missing strains. The complete IC50 data set is presented in Supplementary Table S3.

*Calculation of accessible evolutionary trajectories*

Following previously established methodology (Weinreich et al. 2006, DePristo et al. 2007, Lozovsky et al. 2009), we used the allele-specific resistance (IC50) data to analyze the mutational trajectories that are accessible to DHFR evolution. Under a model where selection acts to increase pyrimethamine resistance, we assumed that the time to fixation or loss of a newly arising mutation is much shorter than the time between mutations ("strong selection/weak mutation;" Gillespie 1984). As alleles with a single mutation do not segregate long enough to experience a second mutation, this model considers evolutionary trajectories with only single, positive mutational steps (see Weinreich et al. 2006 for a detailed description). Following DePristo et al. (2007), we consider all potential positively selected single mutant neighbors, including reversions of previously fixed mutations. We consider only mutations that increase resistance, assuming that probabilities (and thus rates) of fixation will be much higher for such mutations than for neutral mutations or those that decrease resistance.

Because each fixation event is statistically independent of those occurring previously, The probability of moving from the low fitness wild type (*wt*) to an allele of a higher fitness, *dhfr**, via mutational intermediates *a*, *b*, and *c* is given, as in Weinreich et al. (2006), by

$$P_{wt \to dhfr*} = P_{wt \to a} \cdot P_{a \to b} \cdot P_{b \to c} \cdot P_{c \to dhfr*} \ . \quad (1)$$

We used two methods for estimating the probability of fixation ($P_{i \to j}$) of the single mutant neighbor, $j$, of current allele $i$. Under equal fixation probability, we assume that all favorable alleles have an equal probability of fixation. Algebraically,

$$P_{i \to j} = \frac{1}{\left| M_i^+ \right|} \quad (2)$$

where $M_i^+$ is the set of all single mutant neighbors of positive selective value.

Under correlated fixation probability, we follow the extreme value theorem based approach of Weinreich et al. (2006) based on Orr (2002). This model assumes a correlation between the size of the selective increase (in our case, drug resistance) and its fixation probability. In particular,

$$P_{i \to j} = \frac{\sum_{x=r_j}^{r_i - 1} \frac{1}{x}}{\sum_{k \in M_i^+} \sum_{x=r_k}^{r_i - 1} \frac{1}{x}} \quad (3)$$

where $r_i$ is the fitness rank (based on IC50 value) of all alleles regardless of mutational adjacency.

In order to account for the effects of genome-specific mutational bias in *Plasmodium falciparum*, we weight the probability of each potential fixation by its mutational frequency according to the following equation:

$$P_{bias(i\to j)} = \frac{P_{i\to j}\beta_{i\to j}}{\sum_{a\in M_i^+} P_{a\to j}\beta_{a\to j}} \quad (4)$$

where $P_{i\to j}$ is the equal or correlated transition probability as calculated above, and $\beta_{i\to j}$ is the relative bias of the mutation necessary to produce allele *j* from allele *i*. Daniel Neafsey (Broad Institute, Cambridge, MA) kindly provided a twelve-parameter mutation rate matrix based upon 1073 intergenic SNPs in *P. falciparum* (see Table S3 in Lozovsky et al. 2009). SNPs were identified using neighborhood quality standard (NQS) criteria. Eligible SNPs had quality scores of at least Q20 for both alleles and did not occur in CpG dinucleotides. The directionality of mutations was inferred based on simple parsimony with *P. falciparum*'s sister species, *P. reichenowii*.

Probabilities of evolutionary trajectories and their corresponding confidence intervals were estimated using simulations run using PERL. For each allele, we used the calculated IC50 value and the corresponding standard error as the mean and standard deviation of a normal distribution defining the resistance distribution for each allele. Using these IC50 distributions to probabilistically define mutational landscapes, we simulated 1000 mutational landscapes. We then simulated 1 million rounds of evolution on each landscape under both fixation models (see Lozovsky et al. 2009).

Simulating landscapes and trajectories in this way allows the probability estimates to account for uncertainty in our resistance measurements. As a result, many trajectories, regardless of their probability, occur on low-likelihood landscapes. We therefore report a set of consensus trajectories that occur on at least 85% of all landscapes. Changing the percent of simulated landscapes on which a trajectory must occur only modestly changes the number of trajectories

considered (95% threshold = 29; 85% threshold = 46; 50% threshold = 85). However, it does not change the identity of the most frequent trajectories.

Mean trajectory probabilities (see Figure 3.3, Supplementary Table 3.S1) represent the mean frequency of each trajectory across the 1,000 simulated landscapes. Statistics were calculated using scripts written in *R*.

**Results**

In order to understand how various mutational combinations may affect the ability of strains to grow, we analyzed the growth rates of different genotypes in the absence of the antifolate drug (Supplementary Figure S1, Supplementary Table S2). Among the 48 genotypes, 19 demonstrated no observable growth in the absence of pyrimethamine; we consider these alleles to be nonfunctional even though some demonstrate *in vitro* activity toward dihydrofolate (e.g. A16V; see Sirawaraporn et al. 1997). The 29 functional alleles have relative growth rates between 71-104% of the wild type. Among the 6 single-mutant neighbors of the wild-type sequence, 5 have statistically significantly lower growth rates than the wild type (based on non-overlapping 95% confidence intervals; but see 00100 in Supplementary Figure S1). Only C59R has a non-significantly different growth rate. In the yeast system, the wild type allele appears to be a fitness peak in the absence of drug pressure.

We next analyzed the pyrimethamine resistance levels of the 29 functional alleles (Supplementary Figure S2, Supplementary Table S3). We define resistance as the Inhibitory Concentration 50 (IC50), which is the concentration of drug needed to reduce the strain's growth rate by half (see Materials and Methods). Consistent with previous resistance data from parasite field isolates, the quadruple mutant N51I/C59R/S108N/I164L exhibits the highest resistance, and triple mutants C59R/S108N/I164L and N51I/C59R/S108N also exhibit high levels of resistance (Sirawaraporn et al. 1997). ). Likewise, S108N confers the highest resistance among single mutations.

The individual mutations have remarkably different effects on resistance (Table 1). For example, while S108N increases pyrimethamine resistance 128 fold, replacing Ala with Val at site 16 reduces resistance on the vast majority of genetic backgrounds. Mutations also differ in

their ability to restore functionality to a nonfunctional genetic background (see Rescues, Table 1).

Overall, we observe no clear association between resistance level and growth rate (Figure 1). Correlation analysis between growth rate and resistance levels suggests these two phenotypes are independent (Pearson correlation: $P$= 0.7589). This lack of association suggests phenotypic robustness in DHFR evolution in the genetic background of *S. cerevisiae*. Further, neither growth rate nor pyrimethamine resistance is a simple function of the number of mutations present in a DHFR allele (Supplementary Figure S4). Regression analyses between the number of mutations and either phenotype failed to yield a significant relationship (growth rate: adjusted $R^2 = 0.001994$, $P = 0.313$; IC50: adjusted $R^2 = 0.05281$, $P = 0.121$). Our data indicates that only specific combinations of mutations are beneficial to either growth rate or resistance and that interactions between mutations strongly affect phenotype.

In order to understand the effect of this mutational landscape on DHFR evolution, we simulated the evolution of pyrimethamine resistance following previously established methodology (Weinreich et al. 2006, DePristo et al. 2007, Lozovsky et al. 2009, see Methods). Assuming that the time between mutations is much longer than the time for fixation or loss of new mutations (Gillespie 1984, Orr 2002), our simulations move step-by-step through the mutational landscape adding or removing a single mutation at each point along a mutational trajectory. Given the relative likelihood of fixing a neutral or deleterious mutation under the intense selective pressure of antibiotics, we consider only positively selected mutational steps. As it is unclear how the level of resistance to pyrimethamine corresponds to fitness, we use two models to predict the probability of mutational fixations. The equal fixation model assumes that all favorable steps are equally likely, whereas the correlated fixation model assumes that a

mutation's probability of fixation is proportional to the magnitude of the increase in resistance (Weinreich et al. 2006). To compensate for mutational bias in the *P. falciparum* genome, we weight the frequency of the occurrence of mutations by the *P. falciparum*-specific relative mutation rates (see Materials and Methods above, and Table S3 in Lozovsky et al. 2009).

While we observe 46 selectively accessible mutational trajectories (i.e. those in which each step results in an increase in resistance), DHFR evolution is actually highly predictable and dominated by a handful of trajectories. The ten most likely evolutionary trajectories, depicted in Figure 2, are observed between 84% and 99% of the time (Figure 3). Further, over 80% of our simulations fix S108N first (Supplementary Figure S5) and all trajectories end at the global resistance maximum, the quadruple mutant, N51I/C59R/S108N/I164L. Additionally, while many functional genotypes containing A16V have higher pyrimethamine resistances than the wild type, this mutation is not visited in any of the most frequent trajectories. Perhaps because of its extremely detrimental effect on native DHFR function (Sirawaraporn et al. 1997), we observe that A16V is only favorable on 3 of the possible 24 genetic backgrounds (Table 1).

The three most likely evolutionary trajectories illustrate how resistance can evolve without necessarily compromising growth rate. Figure 4 depicts the growth rate and resistance level of alleles at each mutational step in these pathways. The right hand plots for each pathway demonstrate how resistance continuously increases at each step in these paths. However, the left hand plots show that growth rate fluctuates along the path to higher resistance. Linear regression models reveal that mutational step has no significant effect on growth rate over the course of these three trajectories (adjusted $R^2 < 0.05$ and $P > 0.35$ for all three regressions). In each trajectory, subsequent resistance increasing mutations quickly compensate for the growth rate effect of the initial fixation (S108N).

**Discussion**

We describe the growth rate and pyrimethamine resistance mutational landscapes of DHFR and find growth rate remarkably robust to mutations that increase resistance. Correlation analyses and evolutionary simulations reveal that, in the yeast model system, resistance and growth rate phenotypes freely associate. Because interactions between mutations seem to play a large role in determining both growth rate and resistance levels, the phenotype of alleles with multiple mutations is difficult to predict based on the phenotypic effects of the individual mutations alone

In general, there is a complex relationship between different DHFR genotypes' *in vitro* biochemical properties and their organismal phenotypes. For example, the pyrimethamine affinity ($K_i$) of the individual DHFR alleles does predict the level of resistance of each strain (Supplementary Figure S6; Pearson correlation: 0.89, $P = 0.0001$). However, there are exceptions. Some mutations that increase pyrimethamine affinity (decrease $K_i$) still increase resistance (e.g. N51I and I164L; see Supplementary Figure S2 and Sirawaraporn et al. 1997). Even more surprisingly, there is no significant correlation between the native activity of different DHFR alleles and their growth rate (Supplementary Figure S6). For example, while the activity ($k_{cat}/K_M$) of wild type and N51I/C59R/S108N alleles for dihydrofolate differ by nearly 40-fold, they grow at the same rate in the absence of pyrimethamine. The well-established concave relationship between fitness and enzyme activity for pathway enzymes may explain some of the absence of correlation (Hartl et al. 1985); however, this relationship cannot explain cases in which one allele has a higher activity but a lower growth rate than another (e.g., compare N51I with C59R/S108N; Figure 1, Sirawaraporn et al. 1997). We hypothesize that these mutations

affect other protein properties, including degradation, aggregation, and folding, which may also impact growth rate.

Previous research suggests that mode of binding between drug and target may dictate the tradeoff between resistance and native enzyme function (Berkhout et al. 1999, Tawfik 2005). Drugs that bind directly in the active site may impose greater tradeoffs than drugs that bind` external to the catalytic core (Berkhout 1999, Tawfik 2005). Applying this model, antifolate drugs such as pyrimethamine, which bind directly in DHFR's active site and interact with key residues involved in dihydrofolate binding (Yuvaniyama et al. 2003), should impose a strong tradeoff in the development of pyrimethamine resistance. However, while the addition of these mutations significantly decreases the native enzyme activity toward dihydrofolate (Sirawaraporn et al. 1997), they do not have the same, consistent impact on growth rate. In total, our data suggests that organismic fitness, as determined by growth rate, may be even more robust than biochemical parameters alone would indicate.

Despite the additional constraint of maintaining its native enzymatic function, DHFR's evolutionary landscape is similar in one important aspect to that of β–lactamase (Weinreich et al. 2006). As in Weinreich et al. (2006), our simulation results also suggest that protein evolution may be highly biased toward a small number of mutational trajectories. In both cases, between two and four trajectories are likely to occur at least 50% of the time, independent of the fixation model used.

Surprisingly, the DHFR landscape may be more accessible to natural selection than the β–lactamase landscape. To make these landscapes comparable, we limit the mutational landscape to those mutations comprising the global fitness maximum (i.e. five for β–lactamase

and four for DHFR). Further, we consider mutational trajectories that are comprised solely of forward mutations as these may cover as much as 99% of the trajectory probability space (DePristo et al. 2007). Weinreich et al. (2006) observe that 15% to 32.5% (18 to 39 of 120) of forward trajectories are accessible while we observe that 58% (14 of 24) of potential forward trajectories are accessible. The β–lactamase landscape appears more constrained even if the landscape is restricted to the four sites that are likely to fix first (9 of 24 or 37.5%). As growth rate appears to be robust to mutations increasing resistance, our results suggest that the maintenance of an existing enzymatic function does not significantly impact the evolution of nonnative protein functions.

Our results from a yeast system for malarial DHFR are similar to those from a system developed for *Escherichia coli* (Chusacultanachai et al. 2002). As explored by Lozovsky et al. (2009), the favored evolutionary pathways in the *E. coli* system are congruent with those in yeast (heavy lines in Figure 2). Like in the yeast system, the DHFR alleles in *E. coli* show no consistent correlation with growth rate in the absence of drug ($P = 0.81$).

However, the two systems exhibit some notable differences. For example, the variance in growth rate among strains carrying the various DHFR alleles is ~10 times greater in *E. coli* than in yeast. The narrower range of growth rates is reflected in the smaller effects of individual replacements. In *E. coli*, replacing the triple mutant N51I/C59R/S108N with the quadruple mutant N51I/C59R/S108N/I164L reduces growth rate by about 40 percent, and replacing C59R/S108N/I164L with quadruple mutant reduces it by about 32 percent. In yeast, by contrast, the former mutation reduces growth rate by only 14 percent (Figure 4C and D, Figure 4E and F), and the latter mutation has no detectable effect though the standard error bars are quite large (Figure 4A and B). The general amelioration of the growth rate effects of the DHFR allele may reflect a

lower requirement for DHFR activity in yeast relative to *E. coli*. If it exists, this lower DHFR activity requirement may be due to generalized reasons in the metabolic economy of yeast, or it may be due to some specific enzyme such as a relative increase in the activity of GTP-cyclohydrolase I, which in yeast is encoded in *FOL2* (Nardese et al., 1996). This is the first enzyme in the biosynthetic pathway for folic acid, and in *P. falciparum*, Nair et al. (2008) have shown that copy-number polymorphisms can reduce the growth-rate effects of DHFR mutants.

Our results may lend insight into the evolution of *P. falciparum* DHFR in nature. For example, while the vast majority of our constructed alleles are not observed in malarial field isolates, all of the alleles present in each of the three most likely mutational trajectories have been isolated from patients (Sirawaraporn et al. 1997). We also confirm the importance of the S108N mutation, which has long been speculated to be the first mutation fixed in DHFR resistance evolution based predominantly on its biophysical importance (Sirawaraporn et al. 1997, Yuvaniyama et al. 2003). In light of the challenge of culturing and genetically manipulating the parasite itself, the use of this and other model systems may provide powerful insights into combating the threat of drug resistance in *Plasmodium falciparum*.

Negative tradeoffs between growth rate and resistance at drug targets provide hope in combating the evolution of antibiotic resistance. If large negative tradeoffs exist, one might imagine restoring drug susceptibility by relaxing drug pressure (Andersson 2006). However, upon the relaxation of drug pressure, resistance phenotypes are likely to be maintained while additional mutations compensate for their fitness consequences (Maisnier-Paitin et al. 2002, Nair et al. 2008). Our results are consistent with these findings and show that resistance-conferring mutations themselves can compensate for the fitness consequences of initial mutations (Figure 4). Together, these results suggest that once initially selected for, drug resistant genotypes may

remain at high frequencies in populations even in the absence of antibiotic pressure. Resistance prevention may still provide the best strategies in combating antibiotic resistance (Palumbi 2001).

**References**


Aharoni A, Gaidukov L, Khersonsky O, Gould SM, Roodveldt C, Tawfik DS. 2005. The 'evolvability' of promiscuous protein functions. Nat Genet. 37: 73-76.

Andersson DI. 2006. The biological cost of antiobiotic resistance: any practical conclusions?. Curr Opin Microbiol. 9: 461-465.

Berkhout B. 1999. HIV-1 Evolution under Pressure of Protease Inhibitors: Climbing the Stairs of Viral Fitness. J Biomed Sci. 6: 298-305.

Björkman J, Hughes D, Andersson DI. 1998. Virulence of antibiotic-resistant *Salmonella typhimurium*. Proc Natl Acad Sci USA. 95: 3949-3953.

Chusacultanachai S, Thiensathit P, Tarnchompoo B, Sirawaraporn W, Yuthavong Y. 2002. Novel antifolate resistant mutations of *Plasmodium falciparum* dihydrofolate reductase selected in *Escherichia coli*. Mol. Biochem. Parasitol. 120: 61–72.

Currie CR, Scott JA, Summerbell RC, Malloch D. 1999. Fungus-growing ants use antibiotic-producing bacteria to control garden parasites. Nature. 398: 701-704

DePristo MA, Hartl DL, Weinreich DM. 2007. Mutational reversions during adaptive protein evolution. Mol Biol Evol. 24: 1608-1610.

Ekland EH, Fidlock DA. 2007. Advances in understanding the genetic basis of antimalarial drug resistance. Curr Opin Microbiol. 363-370.

Foote SJ, Galatis D, Cowman AF. 1990. Amino acids in the dihydrofolate reductase-thymidilate synthase gene of *Plamodium falciparum* involved in cycloguanil resistance differ from those involved in pyrimethamine resistance. Proc Natl Acad Sci USA. 87: 3014-3017.

Gillespie JH. 1984. Molecular evolution over the mutational landscape. Evolution 38: 1116-1129.

Hackbarth CJ, Kocagoz T, Kocagoz S, Chambers HF. 1995. Point mutations in *Staphylococcus aureus* PBP2 gene affect penicillin-binding kinetics and are associated with resistance. Antimicrob Agents Chemother. 39: 103-106.

Hartl DL, Dykhuizen DE and Dean AM. 1985. Limits of adaptation: the evolution of selective neutrality. Genetics. 111: 655-674.

Hunt SY, Detering C, Varani G, Jacobus DP, Schiehser GA, Shieh HM, Nevchas I, Terpinski J, Sibley CH. 2005. Mol Biochem Parasitol. 144: 198-205.

Joseph SB, Hall DW. 2004. Spontaneous mutations in diploid Saccharomyces cerevisiae: More beneficial than expected. Genetics. 168: 1817-1825.

Khersonsky O, Roodveldt C, Tawfik DS. 2006. Enzyme promiscuity: evolutionary and mechanistic aspects. Curr Opin Chem Biol. 10: 498–508.

Kondrashov FA. 2005. In search of the limits of evolution. Nat Genet. 37: 9-10.

Laible G, Hackenbeck R, Sicard MA, Joris B, Ghuysen JM. 1989. Nucleotide sequences of *pbpX* genes encoding penicillin-binding proteins 2x from *Streptococcus pneumoniae* R6 and a cefotaxime resistant mutant, C506. Mol Microbiol. 3: 1337-1348.

Lozovsky ER, Chookajorn T, Brown KM, Imwong M, Shaw PJ, Kamchonwongpaisan S, Neafsey DE, Weinreich DM, Hartl DL. 2009. Stepwise acquisition of pyrimethamine resistance in the malaria parasite. Proc Natl Acad Sci USA. 106: 12025-12030.

Maplestone RA, Stone MJ, Williams DH. 1992. The evolutionary role of secondary metabolites – a review. Gene. 115: 151-157.

Maisnier-Paitin S, Andersson DI. 2004. Adaptation to the deleterious effects of antimicrobial drug resistance mutations by compensatory evolution. Res Microbiol 155: 360-369.

Maisnier-Paitin S, Berg OG, Liljas L, Andersson DI. 2002. Compensatory adaptation to the deleterious effect of antibiotic resistance in Salmonella typhimurium. Mol Microbiol. 2: 355–366.

Mita T, Tanabe K, Takahashi N (13 co-authors). 2007. Independent evolution of pyrimethamine resistance in *Plasmodium falciparum* isolates in Melanesia. Antimicrob Agents Chemother. 51: 1071-1077.

Nair S, Miller B, Barends M, Jaidee A, Patel J, Mayxay M, Newton P, Nosten F, Ferdig MT, Anderson TJ. 2008. Adaptive copy number evolution in malaria parasites. PLoS Genet. 4: e1000243.

Nardese V, Gütlich M, Brambilla A, Agostoni ML. 1996. Disruption of the GTP-cyclohydrolase I gene in *Saccharomyces cerevisiae*. *Biochem. Biophys. Res. Comm.* 218: 273-279.

Nirmalan N, Wang P, Sims PFG, Hyde JE. 2002. Transcritional analysis of genes encoding enzymes of the folate pathway in the human malaria parasite *Plasmodium falciparum*. Mol Microbiol. 46: 179-190.

Orr HA. 2002. The population genetics of adaptation: The adaptation of DNA sequences. Evolution. 56: 1317-1330.

Schlitzer M. 2007. Malaria Chemotherapeutics Part I: History of Antimalarial Drug Development, Currently Used Therapeutics, and Drugs in Clinical Development. ChemMedChem 2: 944-986.

Sibley CH, Macreadie I. 2001. Novel approaches to tackling malarial drug resistance using yeast. IUBMB Life 52: 285-9.

Sikorski RS, Hieter P. 1989. A system of shuttle vectors and yeast host strains designed for efficient manipulation of DNA in *Saccharomyces cerevisiae*. 122: 19-27

Sirawaraporn W, Sathitkul T, Sirawaraporn R, Yuthavong Y, Santi DV. 1997. Antifolate-resistance mutants of *Plasmodium falciparum* dihydrofolate reductase. Proc Nat Acad Sci USA. 94: 1124-1129.

Tawfik DS. 2005. The evolvability of drug resistance: response to Fernandez. J Biomol Struct Dyn. 22: 617-619

Weinreich DM, Delaney N, Depristo MA, Hartl DL. 2006. Darwinian evolution can follow only very few mutational paths to fitter proteins. Science. 312: 111-114.

Wooden JM, Hartwell LH, Vasquez B, Sibley CH. 1997. Analysis in yeast of antimalarial drugs that target the dihydrofolate reductase of *Plasmodium falciparum*. Mol Biochem Parasitol. 85: 25-40.

Yuthavong Y, Yuvaniyama J, Chitnumsub P, Vanichtananankul J, Chusacultanachai S, Tarnchompoo B, Vilaivan T, Kamchonwongpaisan S. 2005. Malarial (*Plasmodium falciparum*) dihydrofolate reductase-thymidylate synthase: structural basis for antifolate resistance and development of effective inhibitors. Parasitology. 130: 249-259.

Yuvaniyama J, Chitnumsub P, Kamchonwongpaisan S, Vanichtanankul J, Sirawaraporn W, Taylor P, Walkinshaw MD, Yuthavong Y. 2003. Insights into antifolate resistance from malarial DHFR-TS structures. Nat Struct Biol. 10: 357-365.

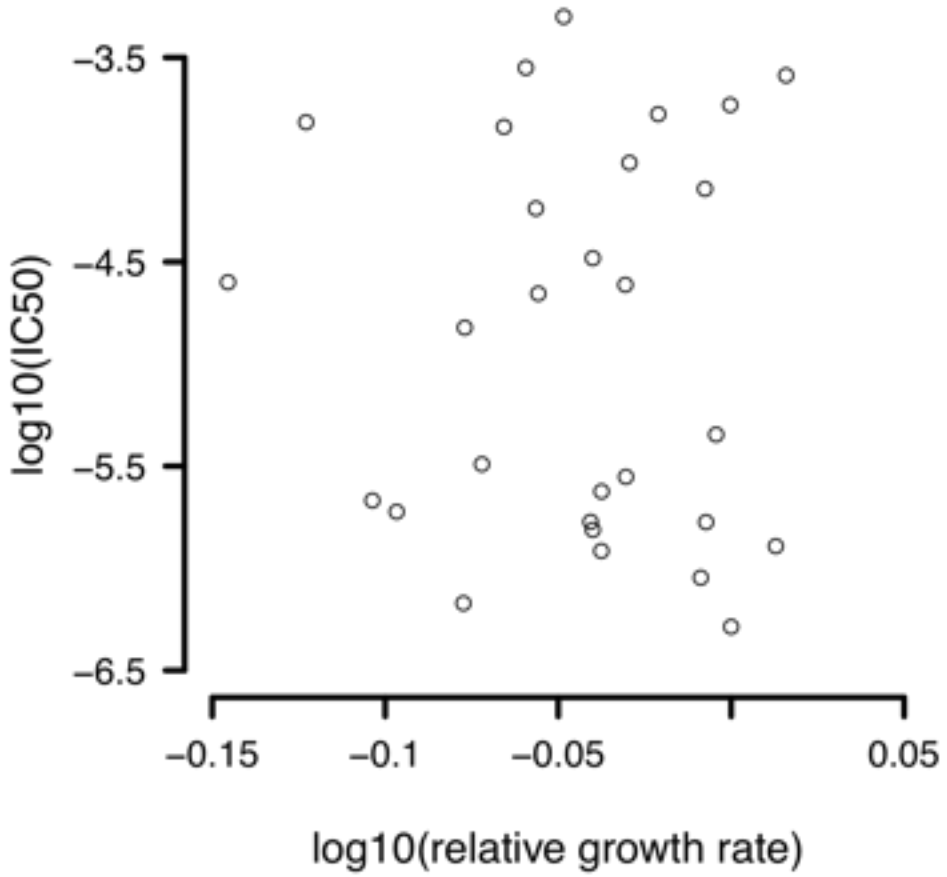


Figure 1. A plot of resistance (IC50) versus growth rate in the absence of pyrimethamine for each of the 29 functional DHFR alleles. No significant correlation exists between these two phenotypes (Pearson correlation: $P = 0.7512$).

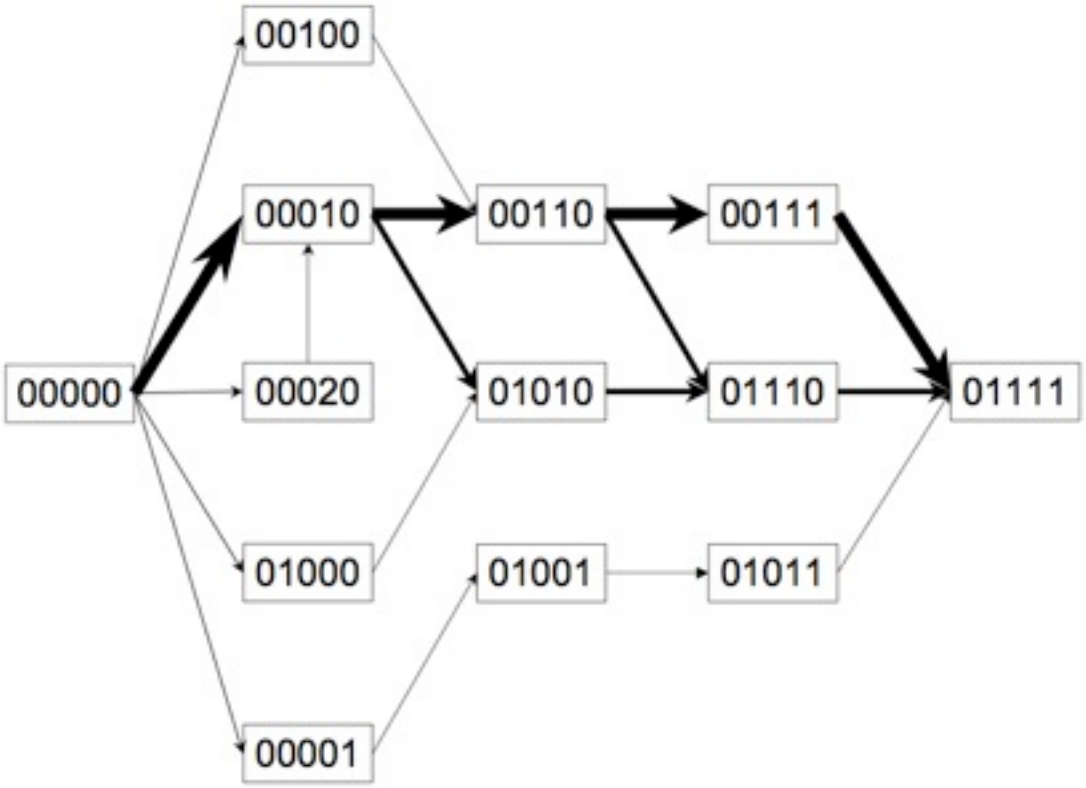


Figure 2. Ten most frequent evolutionary pathways leading from the wild type to the quadruple mutant using the correlated fixation model. According to our model, evolution of pyrimethamine resistance follows one of these 10 pathways nearly 99% of the time. Five digit numbers indicate allelic states at each evolutionary step where each digit corresponds to an amino acid site (from left to right: 16, 51, 59, 108, 164). Wild type states are depicted as 0 while mutant states are depicted as 1 or 2 (site 108: S=0, N=1, T=2). Bold arrows indicate the three most likely pathways and the thickest arrows depicting the most likely path.

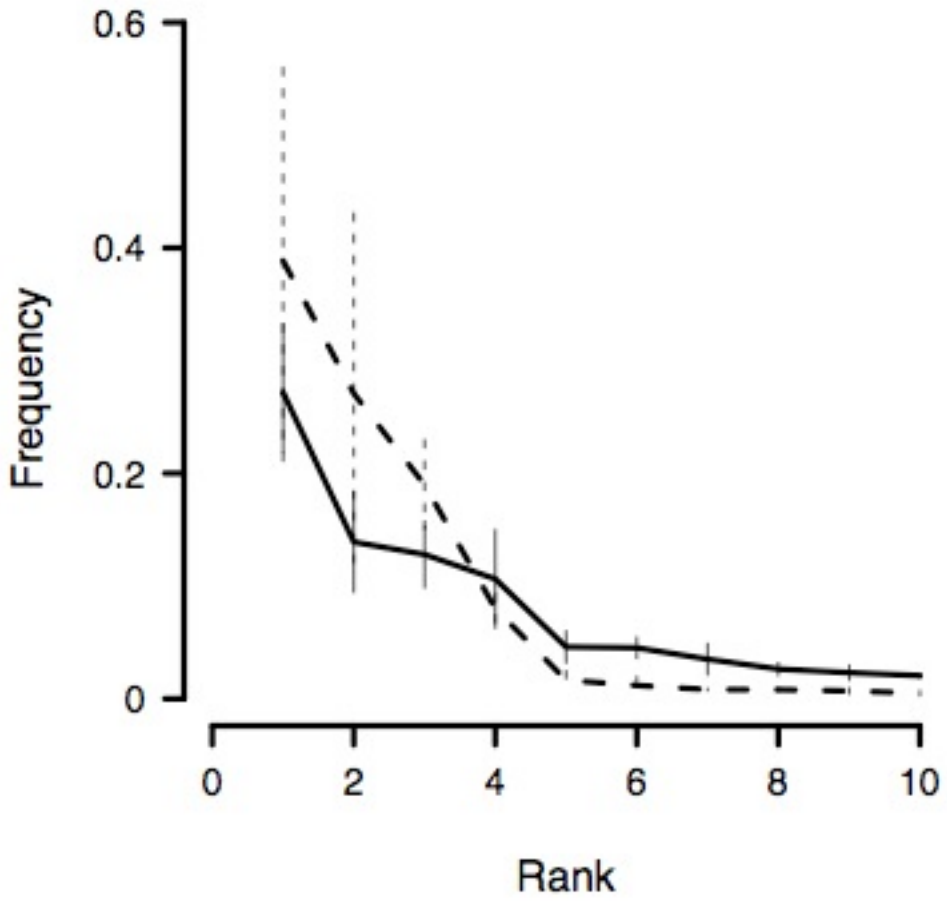


Figure 3. Probability density function (pdf) for ten evolutionary pathways of greatest frequency. The solid line depicts the pdf based on equal fixation probabilities while the dashed line depicts the pdf from correlated fixation probability. Landscapes were simulated based upon IC50 data in Table S3. Pathways are ranked according to mean frequency. Error bars represent 95% confidence intervals.

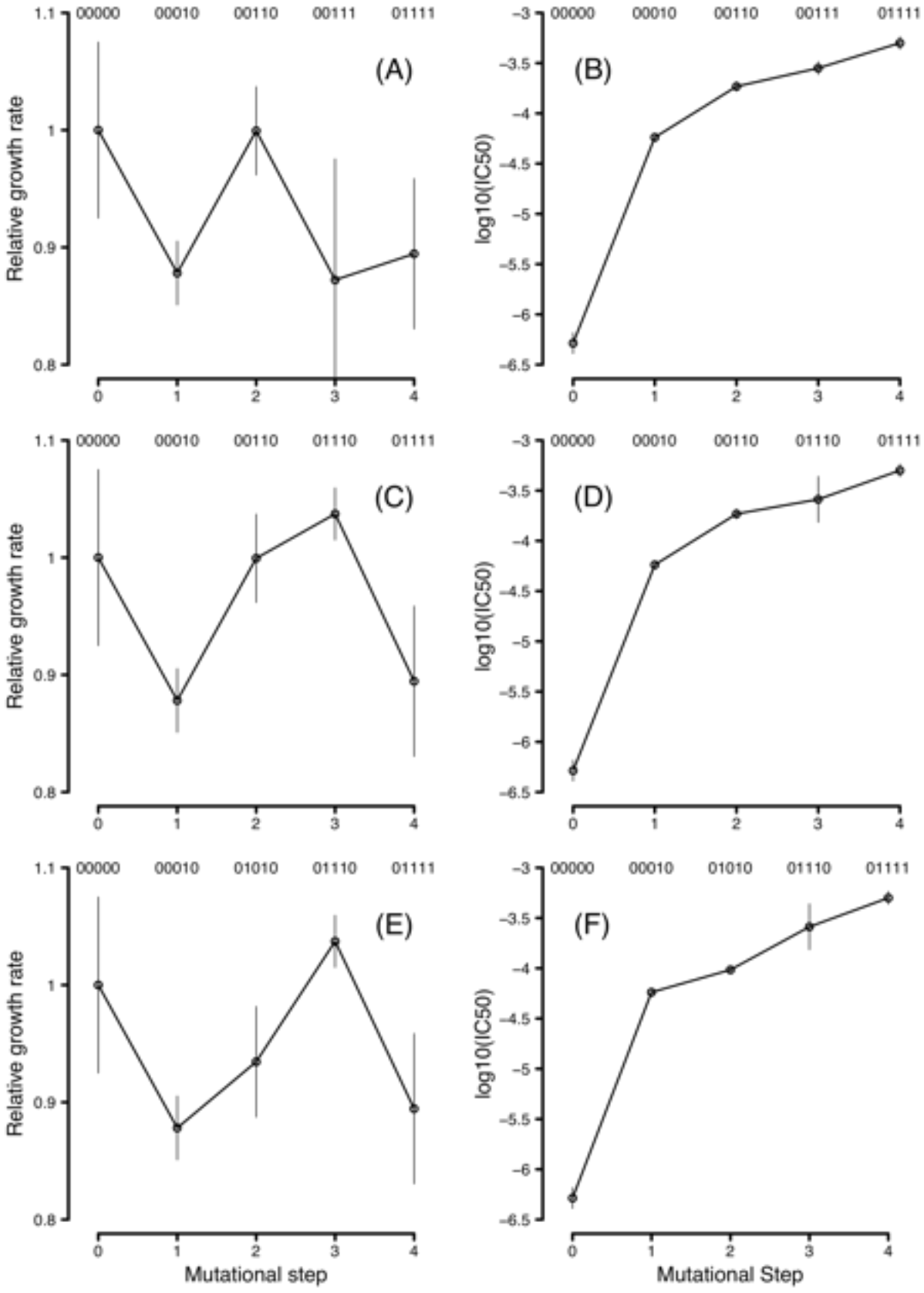
(A)
(B)
(C)
(D)
(E)
(F)
Relative growth rate
log10(IC50)
Mutational step
Mutational Step
00000
00010
00110
00111
01111
01110
01010

Figure 4. Growth rates (left) and resistance values (right) of alleles at each step in the three most likely evolutionary pathways. Plots in the same row (A and B, C and D, E and F) display data from the same trajectory. Alleles at each step in the mutational trajectories are displayed above the plots. Five digit numbers indicate allelic states at each evolutionary step where each digit corresponds to an amino acid site (from left to right: 16, 51, 59, 108, 164). Wild type states are depicted as 0 while mutant states are depicted as 1 or 2 (site 108: S=0, N=1, T=2). Rates represent growth in the absence of drug and are relative to the wild type growth rate. Error bars represent 95% confidence intervals.

Table 1. Summary of mutational effects on pyrimethamine resistance (IC50).

| Mutation | Alleles upon which the mutational effect is Positive[a] | Negative[a] | Negligible | Mean Proportional Increase[b] | Rescues[c] |
|---|---|---|---|---|---|
| A16V | 3 | 20 | 1 | | |
| | | | | 0.28[d] | 2 |
| N51I | 13 | 3 | 8 | | |
| | | | | 1.45 | 2 |
| C59R | 12 | 1 | 11 | | |
| | | | | 3.37 | 5 |
| S108N | 7 | 3 | 6 | | |
| | | | | 128.72 | 0 |
| S108T | 12 | 2 | 2 | | |
| | | | | 52.74 | 4 |
| I164L | 10 | 7 | 7 | | |
| | | | | 2.51 | 3 |

[a] Based on non-overlapping IC50 95% confidence intervals.

[b] Does not include genetic backgrounds where the mutation is deleterious or those where the mutation rescues the ability to grow in unsupplemented YPD (see below).

[c] Number of genetic backgrounds where the presence of the mutation restores the ability to grow in unsupplemented YPD.

[a] Based on one genetic background (C59R + I164L).

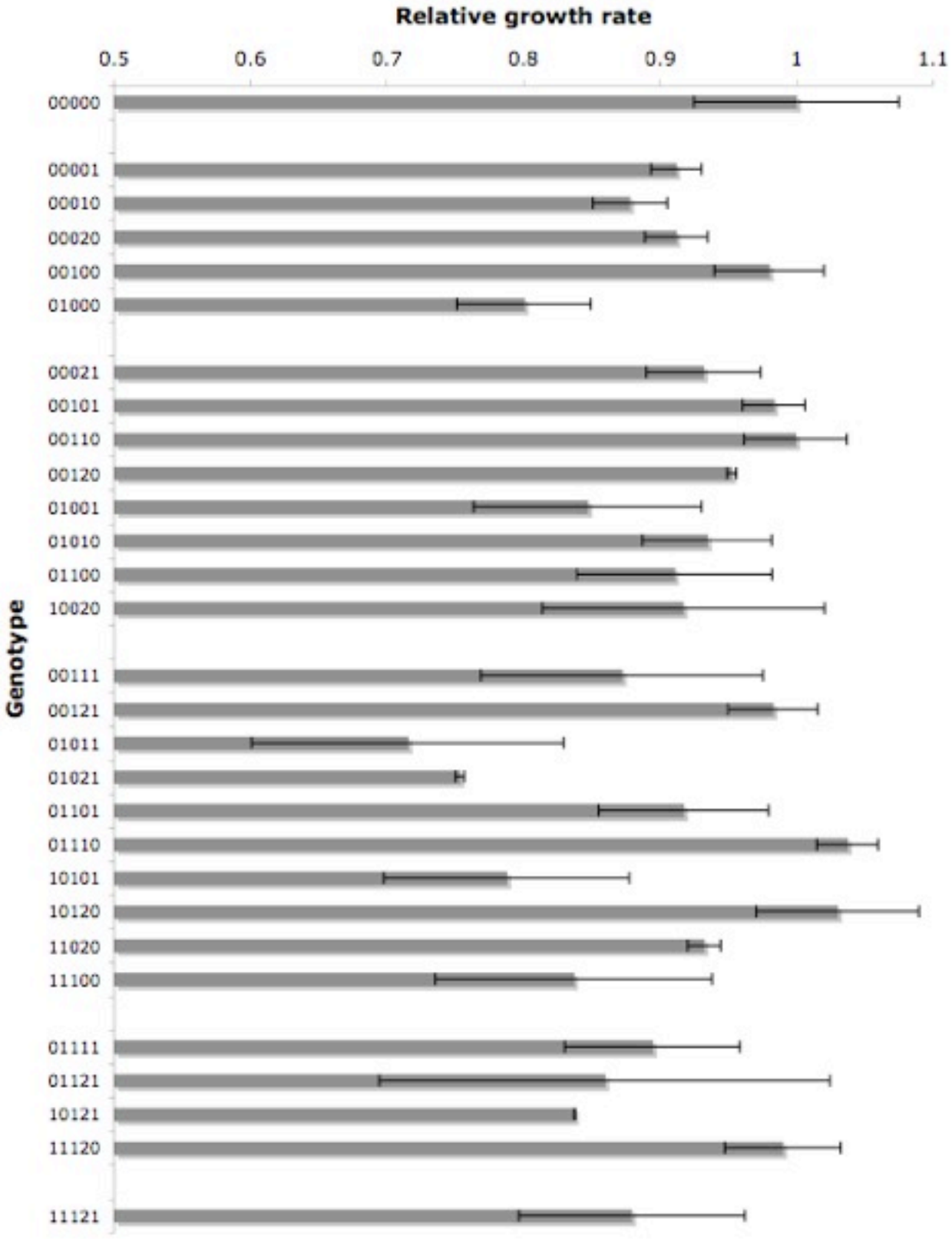
Relative growth rate
0.5
0.6
0.7
0.8
0.9
1
1.1
Genotype
00000
00001
00010
00020
00100
01000
00021
00101
00110
00120
01001
01010
01100
10020
00111
00121
01011
01021
01101
01110
10101
10120
11020
11100
01111
01121
10121
11120
11121

Supplementary Figure S1. Relative growth rate for DHFR alleles. 19 of 48 alleles have no measurable growth in the absence of pyrimethamine and are not depicted. Alleles are designated by code corresponding to the genotype of allele at each of the 5 amino acid sites. 0 indicates the wild type state where a 1 or 2 indicates a mutant state. Sites are designated from left to right as follows: 16, 51, 59, 108 (1=S108N, 2 = S108T), 164. The chart groups alleles together alleles with similar numbers of mutations. Error bars indicate 95% confidence intervals.

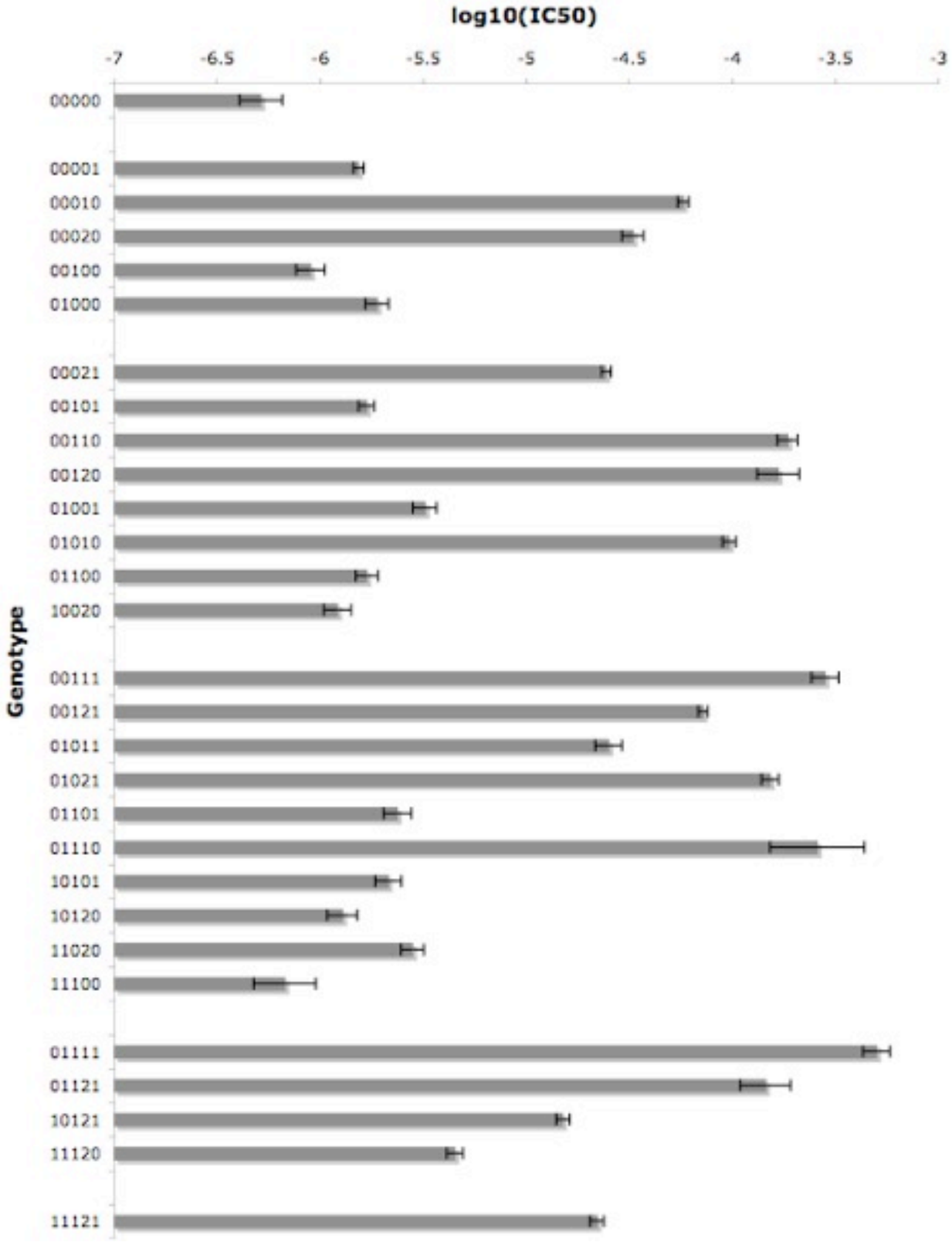
log10(IC50)
-7
-6.5
-6
-5.5
-5
-4.5
-4
-3.5
-3
Genotype
00000
00001
00010
00020
00100
01000
00021
00101
00110
00120
01001
01010
01100
10020
00111
00121
01011
01021
01101
01110
10101
10120
11020
11100
01111
01121
10121
11120
11121

Supplementary Figure S2. Resistance measurements (Inhibitory concentration 50 values) for 29 DHFR alleles with non-zero growth rates in unsupplemented YPD. Alleles are designated as in Figure 1 and are grouped according to number of mutations. Error bars indicate 95% confidence intervals as calculated from IC50 standard errors.

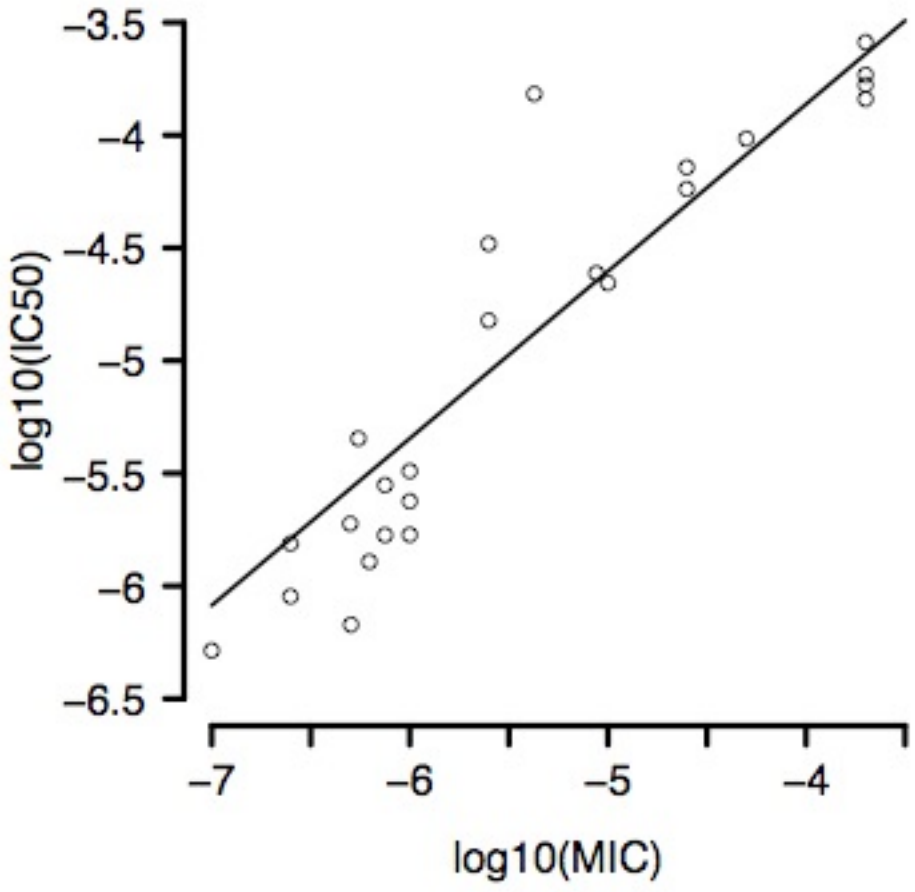


Supplementary Figure S3. Correlation between IC50 values and median MIC values for DHFR alleles (Pearson correlation: $P = 4.383 \times 10^{-11}$).

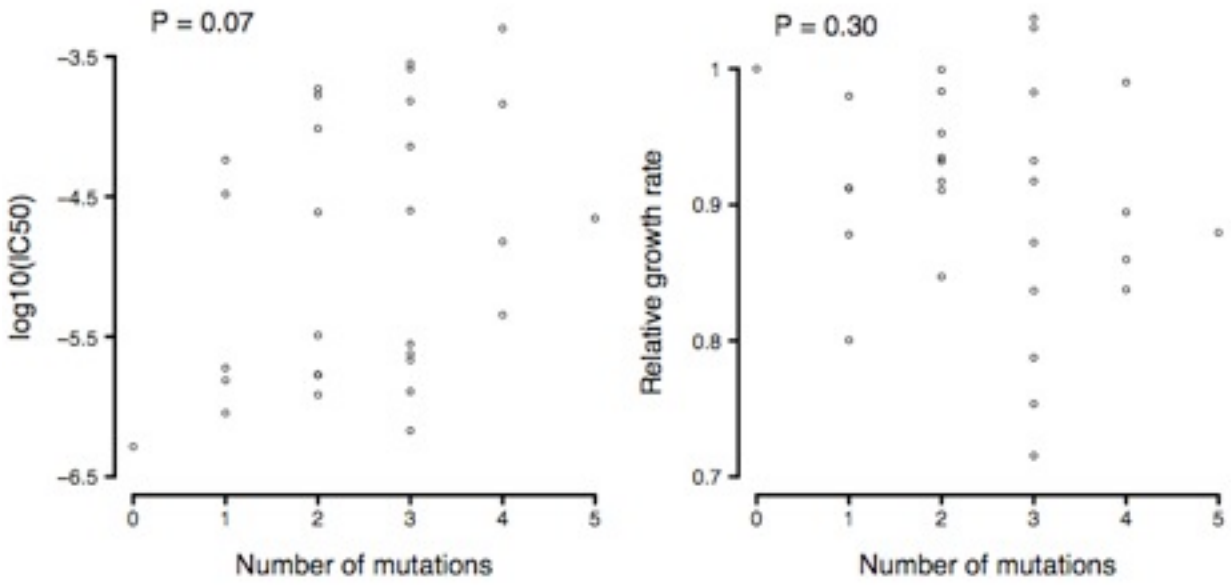


Supplementary Figure S4. Resistance and growth rate phenotypes as a function of the number mutations present in each of the 29 functional DHFR alleles. *P* values shown indicate significance level of Spearman's rank correlations. Inclusion of data points representing the 19 nonfunctional alleles does not affect the significance of the correlation (resistance: $P = 0.93$; growth rate: $P = 0.12$).

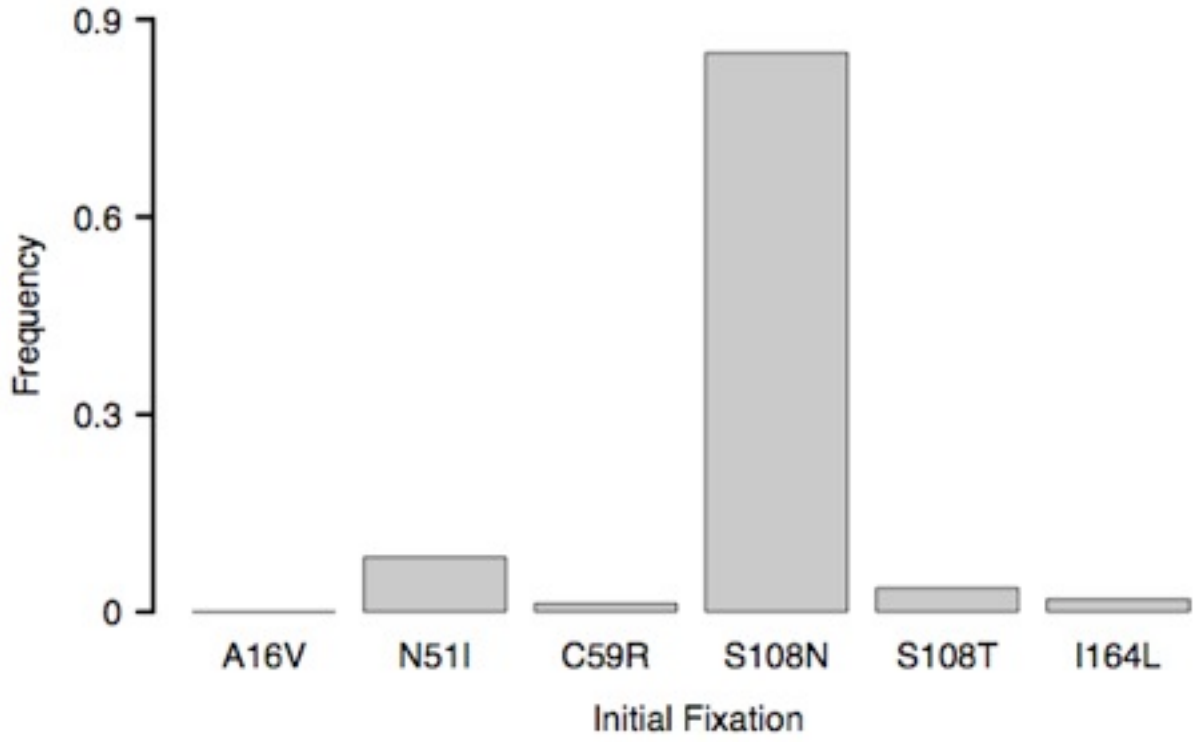


Supplementary Figure S5. Frequency of observing a pathway with a given starting mutation under the correlated fixation probability model. Any given evolutionary pathway has over an 80% chance of beginning with the S108N fixation.

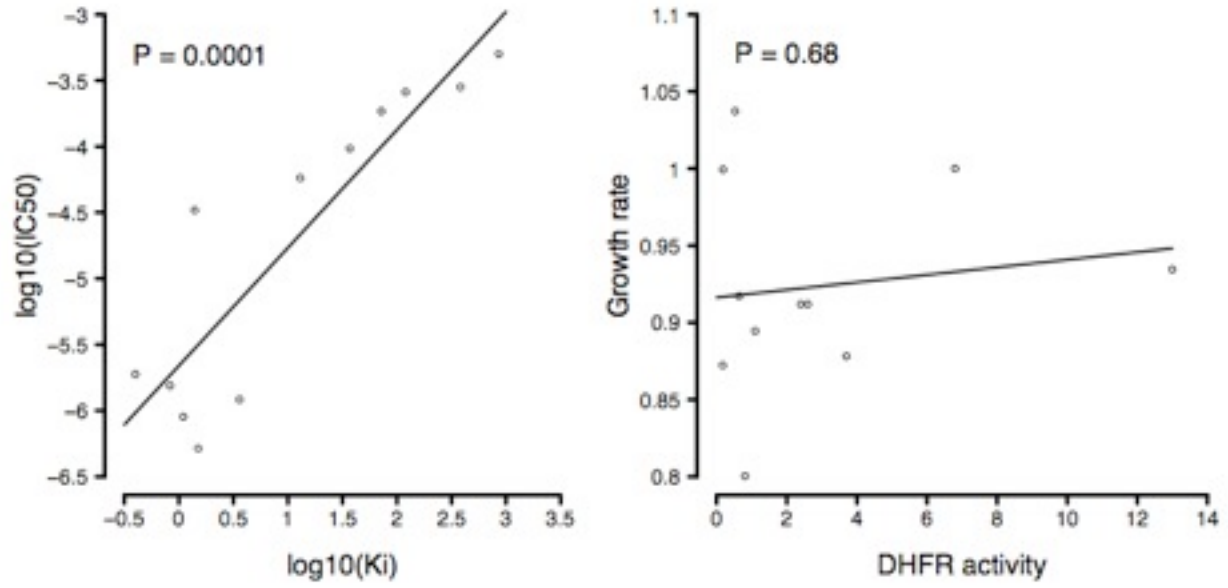


Supplementary Figure S6. Correlation between cellular and biochemical parameters. Left: resistance (IC50) strongly correlates with binding affinity ($K_i$; Pearson correlation: $P = 0.0001$). Right: we observe no relationship between relative growth rate and DHFR activity ($k_{cat}/K_M$; Pearson correlation: $P = 0.68$). Kinetic data from Sirawiraporn et al. (1997).

Supplementary Table S1. Complete list of observed trajectories, their mean realization probability and their standard deviations (SD).

| Trajectory[a] | Correlated Fixation (SD) | Equal Fixation (SD) |
|---|---|---|
| 00000 00010 00110 00111 01111 | 0.38864774 (0.171318377) | 0.139065694 (0.045363128) |
| 00000 00010 00110 01110 01111 | 0.27074593 (0.160082718) | 0.106254998 (0.044355438) |
| 00000 00010 01010 01110 01111 | 0.189791833 (0.040007198) | 0.271743332 (0.061614977) |
| 00000 01000 01010 01110 01111 | 0.079975918 (0.013273888) | 0.128010183 0.030355251 |
| 00000 00020 00010 00110 00111 01111 | 0.016516645 (0.008301096) | 0.02311604 (0.007519723) |
| 00000 00020 00010 00110 01110 01111 | 0.011797008 (0.00791432) | 0.017664455 (0.007375537) |
| 00000 00001 01001 01011 01111 | 0.008141736 (0.00174267) | 0.020511821 (0.002937899) |
| 00000 00020 00010 01010 01110 01111 | 0.008027757 (0.002241096) | 0.045180634 (0.010239161) |
| 00000 00100 00110 00111 01111 | 0.006926104 (0.003389162) | 0.045933575 (0.014961438) |
| 00000 00100 00110 01110 01111 | 0.004857461 (0.003097629) | 0.03508894 (0.014646731) |
| 00000 00001 00021 00121 00111 01111 | 0.004814334 (0.000990451) | 0.006327484 (0.000904467) |
| 00000 00001 00101 00111 01111 | 0.002563139 (0.001308486) | 0.019689391 (0.00486) |

| | |
|---|---|
| 00000 01000 01001 01011 01111 | 0.002396596 (0.000436389) |
| | 0.013328362 (0.001579775) |
| 00000 00001 01001 01011 01010 01110 01111 | 0.001653416 (0.000329423) |
| | 0.026329258 (0.00650709) |
| 00000 00001 00021 00121 01121 01111 | 0.000819277 (0.000538871) |
| | 0.00235375 (0.001608579) |
| 00000 01000 01001 01011 01010 01110 01111 | 0.000487163 (8.71E-05) |
| | 0.017142423 |
| | 0.004073945 |
| 00000 00100 01100 01110 01111 | 0.000362569 (0.000126308) |
| | 0.010866028 (0.003985112) |
| 00000 00100 00101 00111 01111 | 0.000325176 (0.000101816) |
| | 0.009479434 (0.001247647) |
| 00000 00001 00021 00020 00010 00110 00111 01111 | 0.000316136 (0.000169316) |
| | 0.003514894 (0.001241488) |
| 00000 00001 00021 00020 00010 00110 01110 01111 | 0.000231112 (0.000169306) |
| | 0.002676097 (0.001149997) |
| 00000 00001 00101 00121 00111 01111 | 0.000171388 (8.73E-05) |
| | 0.00207069 (0.000513102) |
| 00000 00001 00021 00020 00010 01010 01110 01111 | 0.00015587 (6.02E-05) |
| | 0.006851339 (0.001687122) |
| 00000 00001 00101 10101 10121 00121 00111 01111 | 9.20E-05 (4.31E-05) |
| | 0.005133802 (0.001276927) |
| 00000 00001 00101 01101 01111 | 4.91E-05 (2.23E-05) |
| | 0.002541424 (0.000664341) |
| 00000 00001 00101 00121 01121 01111 | 2.88E-05 (2.32E-05) |
| | 0.000778544 (0.000566009) |
| 00000 00100 00101 00121 00111 01111 | 2.16E-05 (8.12E-06) |
| | 0.000997285 (0.000135864) |

| | |
|---|---|
| 00000 00001 00101 10101 10121 11121 01121 01111 | 2.04E-05 (1.17E-05) |
| | 0.008092047 (0.005902088) |
| 00000 00001 00101 10101 10121 00121 01121 01111 | 1.54E-05 (1.26E-05) |
| | 0.001931447 (0.001408153) |
| 00000 00100 01100 01000 01010 01110 01111 | 1.37E-05 (8.27E-06) |
| | 0.009201777 (0.003962728) |
| 00000 00100 00101 10101 10121 00121 00111 01111 | 1.26E-05 (5.94E-06) |
| | 0.002474674 (0.000335251) |
| 00000 00100 01100 01101 01111 | 7.84E-06 (4.00E-06) |
| | 0.001521393 (0.000498001) |
| 00000 00100 00101 01101 01111 | 6.55E-06 (3.43E-06) |
| | 0.001224385 (0.000193639) |
| 00000 00001 00101 01101 01121 01111 | 3.89E-06 (2.97E-06) |
| | 0.000366587 (0.000267659) |
| 00000 00100 00101 00121 01121 01111 | 3.79E-06 (3.52E-06) |
| | 0.00037406 (0.000257987) |
| 00000 00100 00101 10101 10121 11121 01121 01111 | n.o. |
| | 0.003880744 (0.002674073) |
| 00000 00001 00101 01101 01001 01011 01010 01110 01111 | n.o. |
| | 0.001291951 (0.000428994) |
| 00000 00100 01100 01000 01001 01011 01010 01110 01111 | n.o. |
| | 0.001233807 (0.000533438) |
| 00000 00001 00101 01101 01001 01011 01111 | n.o. |
| | 0.001003871 (0.000261178) |
| 00000 00100 01100 01000 01001 01011 01111 | n.o. |
| | 0.00095229 (0.000362137) |
| 00000 00100 00101 10101 10121 00121 01121 01111 | n.o. |
| | 0.0009268 (0.000638005) |
| 00000 00100 01100 01101 01001 01011 01010 01110 01111 | n.o. |
| | 0.00076847 (0.000289686) |

| | |
|---|---|
| 00000 00100 00101 01101 01001 01011 01010 01110 01111 | n.o. |
| | 0.000622212 (0.000161266) |
| 00000 00100 01100 01101 01001 01011 01111 | n.o. |
| | 0.000602881 (0.000199068) |
| 00000 00100 00101 01101 01001 01011 01111 | n.o. |
| | 0.000483708 (7.63E-05) |
| 00000 00100 01100 01101 01121 01111 | n.o. |
| | 0.000220762 (0.000176643) |
| 00000 00100 00101 01101 01121 01111 | n.o. |
| | 0.000176257 (0.000122652) |

[a]Alleles are designated by code corresponding to the genotype of allele at each of the 5 amino acid sites. 0 indicates the wild type state where a 1 or 2 indicates a mutant state. Sites are designated from left to right as follows: 16, 51, 59, 108 (1=S108N, 2 = S108T), 164.

[b]Not observed.

Supplementary Table S2. Growth rate of 29 functional DHFR alleles in the absence of pyrimethamine.

| Allele | Relative growth rate | Standard Error |
|---|---|---|
| 00000 | 0.000969794 | 3.71E-05 |
| 00001 | 0.000884475 | 9.08E-06 |
| 00010 | 0.000851618 | 1.35E-05 |
| 00020 | 0.000884462 | 1.14E-05 |
| 00021 | 0.000903857 | 2.07E-05 |
| 00100 | 0.000950368 | 1.99E-05 |
| 00101 | 0.000953728 | 1.14E-05 |
| 00110 | 0.000969172 | 1.86E-05 |
| 00120 | 0.000923846 | 1.77E-06 |
| 00111 | 0.000845918 | 5.11E-05 |
| 00121 | 0.000953019 | 1.63E-05 |
| 01000 | 0.000776222 | 2.42E-05 |
| 01001 | 0.000821543 | 4.13E-05 |
| 01010 | 0.000906315 | 2.33E-05 |
| 01011 | 0.000693783 | 5.65E-05 |
| 01021 | 0.000730816 | 1.53E-06 |
| 01100 | 0.000883164 | 3.53E-05 |
| 01101 | 0.000889632 | 3.08E-05 |
| 01110 | 0.001005913 | 1.10E-05 |

| | | |
|---|---|---|
| 01111 | 0.000867504 | 3.17E-05 |
| 01121 | 0.000833688 | 8.17E-05 |
| 10020 | 0.000889515 | 5.10E-05 |
| 10101 | 0.000763795 | 4.45E-05 |
| 10120 | 0.000999062 | 2.95E-05 |
| 10121 | 0.000812232 | 6.95E-08 |
| 11020 | 0.000904206 | 5.88E-06 |
| 11100 | 0.000811488 | 5.01E-05 |
| 11120 | 0.000960132 | 2.11E-05 |
| 11121 | 0.000852969 | 4.10E-05 |

Supplementary Table S3. Inhibitory Concentration 50 (IC50) values for all 29 functional DHFR alleles.

| Allele | $\log_{10}$ (IC50) (M) | Standard Error |
|---|---|---|
| 00000 | -6.286287875 | 0.052603864 |
| 00001 | -5.811815501 | 0.01306476 |
| 00010 | -4.238783454 | 0.014037526 |
| 00020 | -4.48211461 | 0.026490422 |
| 00021 | -4.612314599 | 0.012289668 |
| 00100 | -6.045979852 | 0.035257835 |
| 00101 | -5.774205882 | 0.019191452 |
| 00110 | -3.732112289 | 0.024631581 |
| 00120 | -3.777079714 | 0.051763537 |
| 00111 | -3.55 | 0.033087565 |
| 00121 | -4.14270295 | 0.011584965 |
| 01000 | -5.723515651 | 0.028592668 |
| 01001 | -5.490538213 | 0.029968476 |
| 01010 | -4.015207365 | 0.017167894 |
| 01011 | -4.6 | 0.033087565 |
| 01021 | -3.816615387 | 0.021366234 |
| 01100 | -5.77259696 | 0.027573359 |
| 01101 | -5.624057326 | 0.034434229 |
| 01110 | -3.587469416 | 0.116303605 |
| 01111 | -3.3 | 0.033087565 |

| | | |
|---|---|---|
| 01121 | -3.839352219 | 0.062476174 |
| 10020 | -5.915408591 | 0.033490392 |
| 10101 | -5.668197909 | 0.032062366 |
| 10120 | -5.89185912 | 0.037337574 |
| 10121 | -4.822049854 | 0.016719358 |
| 11020 | -5.55226339 | 0.027819595 |
| 11100 | -6.171380353 | 0.076834 |
| 11120 | -5.345615847 | 0.019982089 |
| 11121 | -4.655746831 | 0.017233065 |

Supplementary Table S4. Median Minimum Inhibitory Concentrations (MIC) for each allele, as determined by solid plate assay.

| Allele | MIC (M) | Standard Deviation |
|---|---|---|
| 00000 | 1.00E-07 | 1.43E-07 |
| 00001 | 2.50E-07 | 1.24E-07 |
| 00010 | 2.50E-05 | 8.84E-06 |
| 00020 | 2.50E-06 | 1.44E-06 |
| 00021 | 8.75E-06 | 8.98E-06 |
| 00100 | 2.50E-07 | 1.54E-07 |
| 00101 | 7.50E-07 | 1.16E-07 |
| 00110 | 2.00E-04 | 4.63E-05 |
| 00111 | 2.00E-04 | 1.125E-04 |
| 00120 | 2.000E-04 | 1.27E-04 |
| 00121 | 2.500E-05 | 1.34E-05 |
| 01000 | 5.000E-07 | 1.34E-07 |
| 01001 | 1.000E-06 | 7.5E-07 |
| 01010 | 5.000E-05 | 1.16E-05 |
| 01011 | 1.000E-05 | 1.71E-13 |
| 01021 | 4.250E-06 | 4.60E-06 |
| 01100 | 1.000E-06 | 6.94E-07 |
| 01101 | 1.000E-06 | 7.75E-07 |
| 01110 | 2.000E-04 | 5.53E-05 |
| 01111 | 4.000E-04 | 2.24E-04 |

| | | |
|---|---|---|
| 01121 | 2.000E-04 | 4.88E-05 |
| 10020 | 5.500E-08 | 4.81E-08 |
| 10101 | 5.500E-08 | 4.84E-07 |
| 10110 | 5.000E-10 | 7.07E-10 |
| 10120 | 6.250E-07 | 3.81E-07 |
| 10121 | 2.500E-06 | 1.66E-06 |
| 11020 | 7.500E-07 | 3.79E-07 |
| 11100 | 5.050E-07 | 5.74E-07 |
| 11120 | 5.500E-07 | 6.36E-07 |
| 11121 | 1.000E-05 | 9.75E-06 |